Interface phonon–polaritons in quantum well systems of polar ternary mixed crystals*

Bao Jin(包 锦)[a)b)] and Liang Xi-Xia(梁希侠)[a)†]

[a)] *Department of Physics, Inner Mongolia University, Hohhot* 010021, *China*
[b)] *College of Science, Inner Mongolia Agricultural University, Hohhot* 010018, *China*

(Received 28 January 2010; revised manuscript received 21 February 2010)

The interface phonon–polaritons in quantum well systems consisting of polar ternary mixed crystals are investigated. The numerical results of the interface phonon–polariton frequencies in the GaAs/$Al_xGa_{1-x}As$, ZnS_xSe_{1-x}/ZnS, and $Zn_xCd_{1-x}Se$/ ZnSe quantum well systems are obtained and discussed. It is shown that there are six branches of interface phonon–polariton modes distributed in three bulk phonon–polariton forbidden bands in the systems. The electric fields of interface phonon–polaritons are also presented and show the interface locality of the modes. The effects of the 'two-mode' and 'one-mode' behaviours of the ternary mixed crystals on the interface phonon–polariton modes are shown in the dispersion curves.

Keywords: interface phonon–polaritons, quantum wells, ternary mixed crystals
PACC: 4110H, 7136, 6350

1. Introduction

Low-dimensional semiconductor systems, such as quantum wells, heterostructures, and superlattices have been investigated extensively due to their applications to new photo-electronic devices. The surface mode and the interface mode of elementary excitations in these systems are of considerable interest in condensed matter physics.[1−13] Surface and interface phonon–polaritons are both the mixed modes coupling the transverse magnetic (TM) modes resulting from the electromagnetic waves with infrared active lattice vibrations localised near the surfaces or interfaces of the systems. These modes can usually be observed by using the Raman scattering and attenuated-total-reflection (ATR) methods experimentally.[1,2,6] Recently, surface and interface phonon–polaritons of wurtzite structure GaN thin film grown on 6H-SiC substrate were investigated by means of p-polarised infrared ATR spectroscopy.[13]

Mills and Maradudin[14] reported the first study of the surface phonon–polaritons in a film on a substrate and indicated that the surface and the interface phonon–polariton frequencies lie between the transverse optical (TO) and longitudinal optical (LO) phonon frequencies of the surface active medium, where the dielectric function is negative. Nakayama *et al.*[15] studied a GaAs/AlAs heterostructure system and obtained a branch of surface modes and four branches of interface modes of phonon–polaritons. Recently, He *et al.*[16] investigated the dispersion equation of interface phonon–polariton modes in a finite superlattice with structure defects by using a transfer matrix method.

There is currently a great deal of interest in the study of properties of the ternary mixed crystals (TMCs), owing to their applications in microwave, photo-electronic, and fast devices.[17−20] The optical vibration of the lattices of TMCs exhibits more complicated characteristic than that in binary crystals,[21,22] and must lead the characteristics of surface and interface phonon–polaritons to be different from each other.

Surface polariton phenomena have already been shown to offer applications in the microscopy,[4,5] coherent thermal emission,[7] surface enhanced infrared absorption,[8] and fields of high-density infrared data storage.[9] The surface and the interface phonon–polaritons in quasi-two-dimensional (2D) systems of polar binary crystals have been investigated extensively.[1−3,6,14−16] However little attention has been paid to the studies on the interface phonon–polaritons in quantum wells (QWs) consisting of polar TMCs. Therefore a detailed investigation on interface phonon–polaritons in QWs is necessary.

In this paper we study theoretically the inter-

*Project supported partly by the National Natural Science Foundation of China (Grant Nos. 10764003 and 10947179).
†Corresponding author. E-mail: xxliang@imu.edu.cn
© 2010 Chinese Physical Society and IOP Publishing Ltd

face phonon–polaritons in QW systems composed of polar TMCs, in the framework of the modified random-element-isodisplacement model[22] and the Born–Huang approximation,[23] based on the Maxwell's equations with boundary conditions. The frequencies and the electric field strengths of the interface phonon–polaritons are calculated and the numerical results for several III–V and II–VI systems are obtained and discussed.

2. Formulation

Consider a QW structure composed of polar TMC materials, where the well layer '1' is in the region of $|z| \leq d$ and the barrier material '2' fills in the regions $|z| > d$. Interface phonon–polaritons propagate along the x direction with the wave vector $\boldsymbol{k}_{\parallel}$. The corresponding electromagnetic interface waves are of transverse magnetic (TM) character and localised near the interfaces of the system, for which the electric field $\boldsymbol{E}$ lies in the x–z plane and the magnetic field $\boldsymbol{H}$ is along the y-axis. Extending the treatment used by Mills and Maradudin[14] for a film of binary crystal to the TMC QW structure, the α-component of the electric field $\boldsymbol{E}$ can be written as the following form:

$$E_\alpha = E_\alpha(z)\exp(\mathrm{i}\boldsymbol{k}_{\parallel}x - \mathrm{i}\omega t), \quad (\alpha = x, z), \tag{1}$$

where

$$E_x(z) = \begin{cases} A^{(0)}\exp\left(-\kappa_2 z\right), & z > d, \\ A^{(1)}\exp(\kappa_1 z) + B^{(1)}\exp(-\kappa_1 z), & -d \leq z \leq d, \\ A^{(2)}\exp\left(\kappa_2 z\right), & z < -d, \end{cases} \tag{1a}$$

where $A^{(0)}$, $A^{(1)}$, $B^{(1)}$ and $A^{(2)}$ describe the amplitudes of the electric fields, κ_1 and κ_2 are the decay constants of the interface waves in the well layer '1' and barrier layer '2', respectively, and both are real and positive to keep the waves decaying with their distances from the interfaces. The equation satisfied by the decay constants is given by

$$\kappa_i^2 = k_{\parallel}^2 - \varepsilon_i\left(\omega\right)\omega^2/c^2, \quad (i = 1, 2). \tag{2}$$

Applying the Maxwell's equations and the continuity boundary condition at $z = d$ and $-d$ to the components $E_\alpha(z)$ of the electric field, the implicit dispersion equation of the interface phonon–polaritons in the QW system can be obtained as

$$\frac{\varepsilon_2\left(\omega\right)}{\varepsilon_1\left(\omega\right)} = \frac{\kappa_2}{\kappa_1}\left[\frac{\exp(-\kappa_1 d) \mp \exp(\kappa_1 d)}{\exp(-\kappa_1 d) \pm \exp(\kappa_1 d)}\right], \tag{3}$$

where the upper one of the plus and minus signs in Eq. (3) is subjected to the higher-frequency branch of polariton modes in the QW system and the down to the lower one. The corresponding dispersion relations are respectively written as

$$\varepsilon_2\left(\omega\right)/\varepsilon_1\left(\omega\right) = -\left(\kappa_2/\kappa_1\right)\tanh\left(\kappa_1 d\right) \tag{4}$$

for the higher-frequency branch, and

$$\varepsilon_2\left(\omega\right)/\varepsilon_1\left(\omega\right) = -\left(\kappa_2/\kappa_1\right)\coth\left(\kappa_1 d\right) \tag{5}$$

for the lower-frequency branch. It is evident from Eqs. (4) and (5) that the interface phonon–polariton waves can propagate only in the region where the ratio of the dielectric function of the well material to that of the barriers is negative, i.e. $\varepsilon_2(\omega)/\varepsilon_1(\omega) < 0$.

The dielectric function $\varepsilon_i(\omega)$ of TMCs can be derived in the framework of the modified random-element-isodisplacement (MREI) model.[22] The Born–Huang-like equation group[23,24] describing the lattice vibrations of TMC systems $\mathrm{A}_x\mathrm{B}_{1-x}\mathrm{C}$ is given by

$$\ddot{\boldsymbol{W}}_1 = b_{11}\boldsymbol{W}_1 + b_{12}\boldsymbol{W}_2 + b_{13}\boldsymbol{E}, \tag{6}$$

$$\ddot{\boldsymbol{W}}_2 = b_{21}\boldsymbol{W}_1 + b_{22}\boldsymbol{W}_2 + b_{23}\boldsymbol{E}, \tag{7}$$

$$\boldsymbol{P} = b_{31}\boldsymbol{W}_1 + b_{32}\boldsymbol{W}_2 + b_{33}\boldsymbol{E}, \tag{8}$$

with $\boldsymbol{W}_1 = \mu_1^{1/2}\boldsymbol{s}_1$ and $\boldsymbol{W}_2 = \mu_2^{1/2}\boldsymbol{s}_2$, where $\boldsymbol{s}_1 = (\boldsymbol{u}_\mathrm{A} - \boldsymbol{u}_\mathrm{C})$ and $\boldsymbol{s}_2 = (\boldsymbol{u}_\mathrm{B} - \boldsymbol{u}_\mathrm{C})$ are respectively the relative displacements of the A–C ion and B–C ion pairs, μ_1 and μ_2 are the corresponding reduced masses, $\boldsymbol{u}_\mathrm{A}$, $\boldsymbol{u}_\mathrm{B}$, and $\boldsymbol{u}_\mathrm{C}$ are the displacements of the ions A, B, and C, respectively. $\boldsymbol{E}$ is the macroscopic electric field and $\boldsymbol{P}$ is the polarisation. The dynamical coefficients b_{ij} $(i, j = 1, 2, 3)$ in the Born–Huang-like equations have been determined by the previous studies.[24,25]

Writing the solutions of Eqs. (6)–(8) as the form of plane-waves with the frequency ω, the relation between the macroscopic electric field $\boldsymbol{E}$ and the polar-

isation $\boldsymbol{P}$ can be obtained as

$$\begin{aligned}\boldsymbol{P} &= \left\{ b_{31}\left[\frac{b_{23}b_{12}-b_{13}\left(b_{22}+\omega^2\right)}{\left(b_{11}+\omega^2\right)\left(b_{22}+\omega^2\right)-b_{12}b_{21}}\right]\right. \\ &+ \left. b_{32}\left[\frac{b_{13}b_{21}-b_{23}\left(b_{11}+\omega^2\right)}{\left(b_{11}+\omega^2\right)\left(b_{22}+\omega^2\right)-b_{12}b_{21}}\right]+b_{33}\right\}\boldsymbol{E}. \end{aligned} \tag{9}$$

And then the dielectric function of the TMC is written as

$$\varepsilon\left(\omega\right)=1+\chi\left(\omega\right)/\varepsilon_0, \tag{10}$$

where

$$\begin{aligned}\chi(\omega) &= \left\{ b_{31}\left[\frac{b_{23}b_{12}-b_{13}\left(b_{22}+\omega^2\right)}{\left(b_{11}+\omega^2\right)\left(b_{22}+\omega^2\right)-b_{12}b_{21}}\right]\right. \\ &+ \left. b_{32}\left[\frac{b_{13}b_{21}-b_{23}\left(b_{11}+\omega^2\right)}{\left(b_{11}+\omega^2\right)\left(b_{22}+\omega^2\right)-b_{12}b_{21}}\right]+b_{33}\right\} \end{aligned} \tag{11}$$

and ε_0 is the vacuum dielectric constant.

Equations (4) and (5) can be solved numerically, by using Eq. (10) with expression (11) for the dielectric functions of the TMC layers in the QW system, to obtain the frequencies of the interface phonon–polaritons each as a function of the 2D wave vector $k_{\parallel}$.

3. Numerical results and discussion

The numerical calculations for the frequencies and the electric field strengths of the interface phonon–polaritons in several TMC QW systems of III–V, II–VI compound semiconductors have been performed. For the convenience of statement, two types of QWs, where TMC $A_xB_{1-x}C$ fills in the well and the barriers, separately, are considered in the calculations. The following formula for the dielectric function $\varepsilon_{\rm b}(\omega)$ of the binary crystal has been used:

$$\varepsilon_{\rm b}\left(\omega\right)=\varepsilon_{\infty}\frac{\omega^2-\omega_{\rm LO}^2}{\omega^2-\omega_{\rm TO}^2}, \tag{12}$$

where ε_{∞} is the optical dielectric constant, and $\omega_{\rm TO}$ and $\omega_{\rm LO}$ are respectively the frequencies of the transverse optical (TO) and longitudinal optical (LO) phonons of the binary crystal.

The numerical results for the $GaAs/Al_xGa_{1-x}As$, ZnS_xSe_{1-x}/ZnS, and $Zn_xCd_{1-x}Se/ZnSe$ QW systems, as examples, are shown in Figs. 1–4. The parameters used in the computations for binary materials are given in Table 1. The TMC TO and LO phonon frequencies are calculated by the method of Ref. [25] and listed in Table 2.

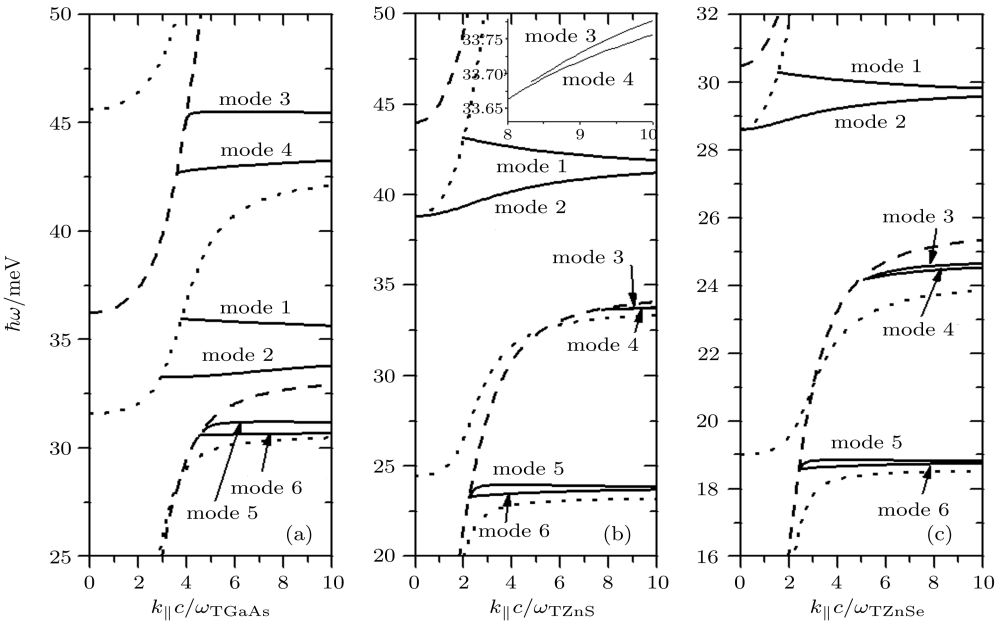


Fig. 1. Energies of interface phonon–polaritons each as a function of wave-vector $k_{\parallel}$ for QW systems (a) $GaAs/Al_{0.35}Ga_{0.65}As$, (b) $ZnS_{0.4}Se_{0.6}/ZnS$, and (c) $Zn_{0.4}Cd_{0.6}Se/ZnSe$ with well layer half-thickness $d = 50$ nm (solid lines). The dimensionless wave-vectors $k_{\parallel}c/\omega_{\rm TGaAs}$, $k_{\parallel}c/\omega_{\rm TZnS}$, and $k_{\parallel}c/\omega_{\rm TZnSe}$ are used, where $\omega_{\rm TGaAs}$, $\omega_{\rm TZnS}$, and $\omega_{\rm TZnSe}$ are the frequencies of TO phonons for GaAs, ZnS, and ZnSe and c the velocity of light. Energies of the bulk phonon–polaritons of binary crystals (long-dash lines) and TMCs (dot lines) are also plotted for comparison.

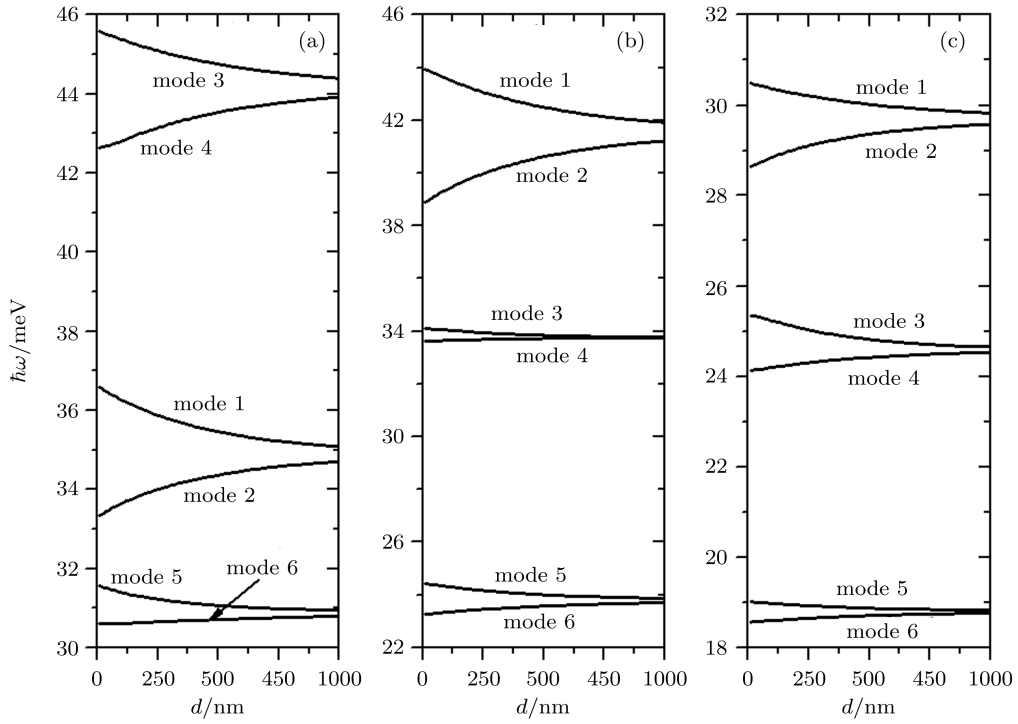


Fig. 2. Energies of interface phonon–polariton modes each as a function of well layer half-thickness d for the QW systems (a) $GaAs/Al_{0.35}Ga_{0.65}As$, (b) $ZnS_{0.4}Se_{0.6}/ZnS$, and (c) $Zn_{0.4}Cd_{0.6}Se/ZnSe$.

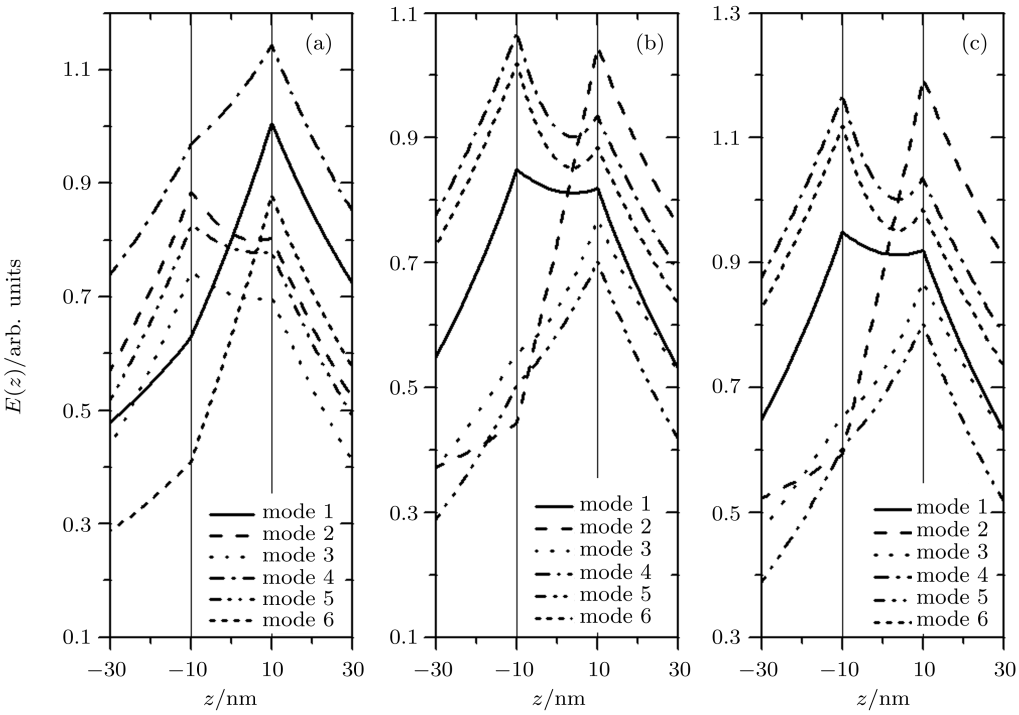


Fig. 3. Spatial dependences of electric field strength of the interface phonon–polaritons for QW systems (a) $GaAs/Al_{0.35}Ga_{0.65}As$, (b) $ZnS_{0.4}Se_{0.6}/ZnS$, and (c) $Zn_{0.4}Cd_{0.6}Se/ZnSe$ with well layer half-thickness $d = 10$ nm for $k_{\parallel} = 20 \times 10^3$ cm^{-1}.

Figures 1(a)–1(c) show the interface phonon–polariton energies each as a function of two-dimensional wavenumber $\boldsymbol{k}_{\parallel}$ for QW systems $GaAs/Al_{0.35}Ga_{0.65}As$, $ZnS_{0.4}Se_{0.6}/ZnS$, and $Zn_{0.4}Cd_{0.6}Se/ZnSe$, respectively. It is found that there are six branches of interface phonon–polariton frequencies, located respectively in the three forbidden bands of bulk phonon–polaritons between the LO and the TO frequencies in the binary crystals and

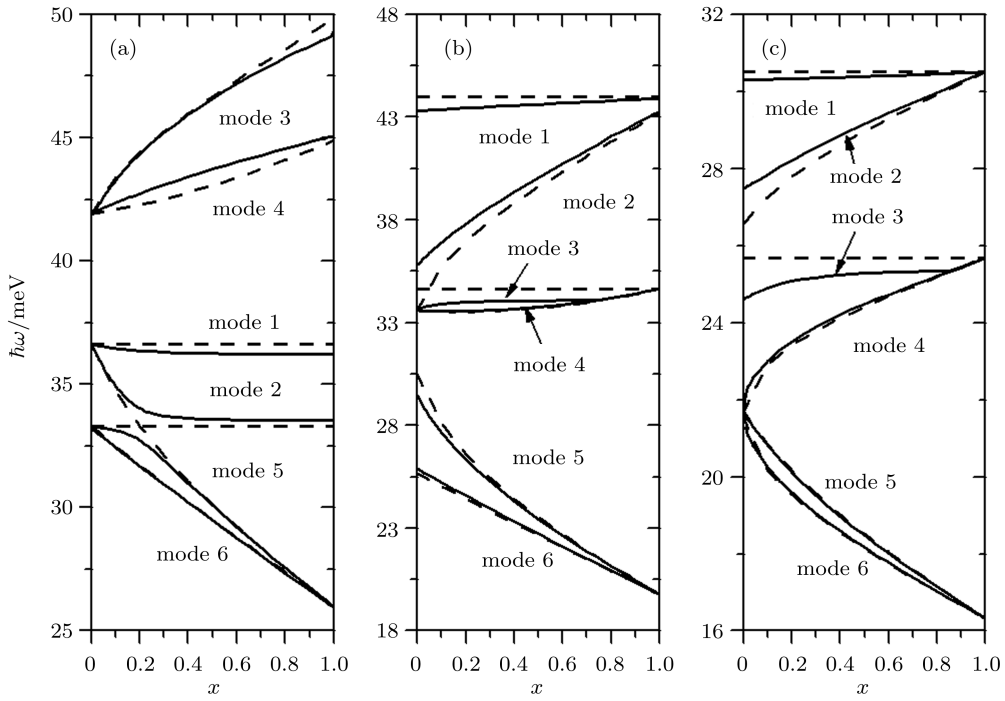


Fig. 4. Energies of interface phonon–polaritons (solid lines) each as a function of composition x for QW systems (a) GaAs/$Al_xGa_{1-x}As$, (b) ZnS_xSe_{1-x}/ZnS, and (c) $Zn_xCd_{1-x}Se$/ZnSe. The dash lines denote the energies of long-wavelength TO and LO phonons subjected to the bulk binary crystals and TMCs.

Table 1. Optical phonon energies, optical dielectric constants, ion masses (M), and the lattice constants (a) for binary materials. Energy is measured in meV, and the lattice constants in nm.

materials	$\hbar\omega_{TO}$	$\hbar\omega_{LO}$	ε_∞	M/arb. units	a
AlAs[a]	44.88	50.09	8.16	26.99 74.92	0.5660[c]
GaAs[a]	33.29	36.25	10.89	69.72 74.92	0.56419[c]
ZnSe[b]	25.67	30.50	5.9	65.38 78.9	0.5668[c]
CdSe[b]	21.52	26.56	6.1	112.4 78.9	0.5993
ZnS[b]	34.65	44.00	5.14	65.38 32.06	0.5410[c]

[a]Ref. [26], [b]Ref. [27], [c]Ref. [28].

Table 2. Optical phonon energies of TMCs measured in meV.

material	$\hbar\omega_{1L}$	$\hbar\omega_{1T}$	$\hbar\omega_{2L}$	$\hbar\omega_{2T}$
$Al_{0.35}Ga_{0.65}As$	31.59	30.59	45.62	42.64
$Zn_{0.4}Cd_{0.6}Se$	19.01	18.55	28.61	24.12
$ZnS_{0.4}Se_{0.6}$	24.44	23.24	38.82	33.62

the LO-TO mode pairs in TMCs, respectively, similar to those in bi-layer systems of TMCs.[29] However, the dispersion curves of the phonon–polaritons in QW systems display quite different characteristics from the later.

The six branches of interface phonon–polariton modes are labeled by numbers 1–6 in Fig. 1, where '1' and '2' are respectively the branches of interface modes with higher-frequency and lower-frequency localised in the forbidden band for bulk phonon–polaritons between ω_{TO} and ω_{LO} of the binary material. Branches '3-4' and branches '5-6' are embedded in the two forbidden bands of bulk phonon–polariton modes between ω_{2T} and ω_{2L} (higher TO-LO pair) and between ω_{1T} and ω_{1L} (lower TO-LO pair) of the TMC, respectively. The frequencies of the six branches of interface phonon–polaritons tend to the three limit values of interface-optical (IO) phonon modes, as the wave-number is large enough, which can be calculated from the following equation:

$$\varepsilon_1(\omega) + \varepsilon_2(\omega) = 0, \tag{13}$$

and the results labeled as ω_{1S}, ω_{2S}, and ω_{3S} are listed in Table 3.

Table 3. Calculated interface optical phonon energies for several QW systems consisting of ternary mixed crystals. Energy is measured in meV.

material	$\hbar\omega_{1S}$	$\hbar\omega_{2S}$	$\hbar\omega_{3S}$
GaAs/$Al_{0.35}Ga_{0.65}As$	34.80	30.93	44.24
$Zn_{0.4}Cd_{0.6}Se$/ZnSe	29.71	24.72	18.80
$ZnS_{0.4}Se_{0.6}$/ZnS	41.61	33.94	23.79

It is expected that the dispersive characteristics

of interface phonon–polaritons depend strongly on the relative values of the TO and LO phonon frequencies in the binary crystal and TMC. The calculated systems can be divided into two types according to the values of TO and LO phonons similar to those in the bi-layer system case:[29]

A: $\omega_{1T} < \omega_{1L} < \omega_{TO} < \omega_{LO} < \omega_{2T} < \omega_{2L}$,
B: $\omega_{1T} < \omega_{1L} < \omega_{2T} < \omega_{TO} < \omega_{2L} < \omega_{LO}$.

The GaAs/$Al_{0.35}Ga_{0.65}$As QW system in Fig. 1(a) falls into case A. The mode curves start from the frequencies of bulk phonon–polaritons in GaAs and $Al_{0.35}Ga_{0.65}$As at the small wave vector $k_{\|}$ and finally have a tendency to reach the IO-phonon frequencies ω_{1S}, ω_{2S}, and ω_{3S} at the large wave vector. It is found that two branches of modes (1 and 2) are localised in the forbidden band of bulk phonon–polariton modes between the LO and the TO frequencies of GaAs. The other two groups of interface phonon–polariton modes: pair 3-4 and pair 5-6, lie in the forbidden bands of AlAs-like (the upper, ω_{2T}–ω_{2L}) and GaAs-like (the lower, ω_{1T}–ω_{1L}) bulk phonon–polariton modes of $Al_{0.35}Ga_{0.65}$As, respectively, where the ratio of the dielectric function ε_2 (ω) to ε_1 (ω) is negative.

On the other hand, the $ZnS_{0.4}Se_{0.6}$/ZnS and $Zn_{0.4}Cd_{0.6}$Se/ZnSe systems belong to case B. In this case, the forbidden band (ω_{TO}–ω_{LO}) for phonon–polariton modes of the binary crystal overlaps with the upper forbidden band (ω_{2T}–ω_{2L}) of the TMC, according to the relation $\omega_{2T} < \omega_{TO} < \omega_{2L} < \omega_{LO}$. As mentioned above, the interface phonon–polariton waves exist only if the relation ε_2 (ω)/ε_1 (ω) < 0 holds. Therefore there are no interface waves propagating in the overlapping frequency region ω_{TO}–ω_{2L}, where the ratio of dielectric function ε_2 (ω)/ε_1 (ω) is positive. At the same time, there are two branches of phonon–polariton modes (modes 3 and 6) in the ZnS/$ZnS_{0.4}Se_{0.6}$ and the ZnSe/$Zn_{0.4}Cd_{0.6}$Se bi-layer systems in the above-mentioned frequency interval.[30] The two groups of interface phonon–polariton modes, i.e., branches '1-2' and branches '3-4', lie respectively in the regions ω_{2L}–ω_{LO} and ω_{2T}–ω_{TO}, except for the mode pair '5-6' situated in the lower forbidden band (ω_{1T}–ω_{1L}) of the TMC. Moreover, Figs. 1(b) and 1(c) show that mode 1 is stopped by the dispersion curves of bulk phonon–polaritons in TMC systems at the small wave vector, and modes 3, 4, 5, and 6 lie in the right of the dispersion curves of bulk phonon–polaritons of the binary crystals, however, mode 2 commences from the LO frequency ω_{2L} of the TMC system with a vanishing wave vector. The interface modes finally converge and tend to the IO-phonon frequencies ω_{1S}, ω_{2S}, and ω_{3S} when the wave vectors are large enough.

It is also deduced that all six branches of interface phonon–polariton modes may not be observed easily due to the very different widths of forbidden bands of TMC systems. The branches 1 and 2 are located in the wider forbidden bands of bulk phonon–polaritons of the binary crystals (3.0 meV for GaAs, 5.18 meV for ZnS, and 1.89 meV for ZnSe), so that they can be separated obviously from each other in frequency and easily observed for either GaAs/$Al_{0.35}Ga_{0.65}$As system or $ZnS_{0.4}Se_{0.6}$/ZnS and $Zn_{0.4}Cd_{0.6}$Se/ZnSe systems. As for the other four branches of interface modes, the two forbidden bands of bulk TMC polaritons in the GaAs/$Al_{0.35}Ga_{0.65}$As system are both wider, so that the interface modes in the bands may be observed, and the 'two-mode' behaviour appears; but the width of the lower forbidden band is only around 1.0 meV (GaAs-like), i.e. one third of the upper band (around 3.0 meV for AlAs-like) for $Al_{0.35}Ga_{0.65}$As. As a result one can infer that mode pair '3-4' in the GaAs/$Al_{0.35}Ga_{0.65}$As system is expected to be easily observed, but mode pair '5-6' is difficult to observe.

Otherwise, the mode pairs '3-4' and '5-6' are respectively in the frequency intervals ω_{2T}–ω_{TO} and ω_{1T}–ω_{1L} for the $ZnS_{0.4}Se_{0.6}$/ZnS and $Zn_{0.4}Cd_{0.6}$Se/ZnSe systems. The widths of two interface mode regions in the $ZnS_{0.4}Se_{0.6}$/ZnS system are narrow (around 1.03 meV and 1.20 meV respectively), and compel the frequencies of modes 3 and 4 as well as 5 and 6 to lie close to each other. Thereupon, on can guess that the four modes (pairs 3-4 and 5-6) are difficult to observe experimentally, particularly for mode pair '3-4'. As for the $Zn_{0.4}Cd_{0.6}$Se/ZnSe system, $Zn_{0.4}Cd_{0.6}$Se shows the typical 'one-mode' behaviour, and the widths for the corresponding regions are calculated to be 1.55 meV and 0.46 meV, respectively. It follows that mode pair '3-4' may be observable although difficult, but the other pair '5-6' in a very-narrow band cannot be observed.

To understand the dependence of interface phonon–polariton frequency on the structure of the QW system, we have also calculated the energies of the interface modes each as a function of the half-thickness d of the well in the above-mentioned QW system, where the wave vector is chosen as $k_{\|} = 80 \times 10^3$ cm^{-1}[13] for definition, and the results are

shown in Fig. 2.

It is seen that the six branches of interface phonon–polariton modes are clearly divided into three groups: mode pairs '1-2', '3-4' and '5-6'. The frequencies of the higher-branches (modes 1, 3, and 5) in the groups have their maxima, while the lower-branches (modes 2, 4, and 6) reach their minima at $d \to 0$. The frequencies of two branches in a group draw to each other with the increase of the well thickness, and finally tend to the IO-phonon frequencies (ω_{1S}, ω_{2S}, or ω_{3S}), the same as those in the single-interface system between the corresponding semi-infinite binary and TMC media, when the well-width is large enough. It follows that the geometrical structures of QWs influence obviously the frequencies of interface phonon–polariton modes.

For giving a pellucid explanation for the locality of the interface mode, we have illustrated the computed spatial distribution of the electric field strengths, $\boldsymbol{E}(z)$, of six interface phonon–polariton modes for the GaAs/$Al_{0.35}Ga_{0.65}$As, $ZnS_{0.4}Se_{0.6}$/ZnS, and $Zn_{0.4}Cd_{0.6}$Se/ZnSe QWs with the half-thicknesses $d = 10$ nm and the wave vector $k_{\|} = 20 \times 10^3$ cm^{-1}[13] in Fig. 3. As expected, modes 1, 4, and 6 are localised in the vicinity of the interface of $z = 10$ nm between GaAs and $Al_{0.35}Ga_{0.65}$As, but the other three modes (2, 3, and 5) are localised at another interface of $z = -10$ nm, for the GaAs/$Al_{0.35}Ga_{0.65}$As QW. The electric fields of interface phonon–polaritons decay rapidly from the corresponding interfaces. A similar situation arises for the $ZnS_{0.4}Se_{0.6}$/ZnS and $Zn_{0.4}Cd_{0.6}$Se/ZnSe systems, where modes 2, 3, and 5 are localised in the interface of $z = 10$ nm, but modes 1, 4, and 6 in other interface ($z = -10$ nm).

To understand the composition effect of TMCs, the energies of the interface phonon–polariton modes each as a function of composition x for GaAs/Al_xGa_{1-x}As, ZnS_xSe_{1-x}/ZnS, and Zn_xCd_{1-x}Se/ZnSe systems have been numerically computed and the results are plotted in Fig. 4. It is apparent that the energies of the interface phonon–polariton modes increase or decrease nonlinearly with composition increasing. The one- and two-mode behaviours of TMCs are also displayed in the interface phonon–polariton modes. The one-mode behaviour of TMC Zn_xCd_{1-x}Se can be comprehended from curves 5 and 6 for the Zn_xCd_{1-x}Se/ZnSe QW system in Fig. 4(c), where the energies of two branches of bulk optical phonons in the TMC are very close to each other, so that the mode pair cannot be observed. Certainly the two-mode behaviours are discovered for the GaAs/Al_xGa_{1-x}As and ZnS_xSe_{1-x}/ZnS separately.

4. Conclusion

We investigate theoretically the interface phonon–polaritons in QW system consisting of polar TMCs in the MREI model and the Born–Huang approximation. As examples, the numerical results for the dispersive curves and the electric fields of the interface phonon–polaritons in several binary/ternary QW systems are given and discussed. It is found that there are six branches of interface phonon–polaritons localised in the vicinities of the interfaces, whose frequencies are embedded in the forbidden bands for bulk polariton frequencies of the layer materials. The observable properties of the six branches of interface phonon–polaritons are related to the widths of the forbidden bands. The effects of the 'two-mode' and 'one-mode' behaviours of TMCs are also shown in the interface phonon–polariton curves.

References

[1] Evans D J, Ushioda S and McMullen J D 1973 *Phys. Rev. Lett.* **31** 369

[2] Marschall N and Fischer B 1972 *Phys. Rev. Lett.* **28** 811

[3] Wendler L and Jäger E 1983 *Phys. Status Solidi* B **120** 235

[4] Wilde Y D, Formanek F, Carminati R, Gralak B, Lemoine P A, Joulain K, Mulet J P, Chen Y and Greffet J J 2006 *Nature* **444** 740

[5] Taubner T, Korobkin D, Urzhumov Y, Shvets G and Hillenbrand R 2006 *Science* **313** 1595

[6] Torii K, Koga T, Sota T, Azuhata T, Chichibu S F and Nakamura S 2000 *J. Phys.*: *Condens. Matter* **12** 7041

[7] Greffet J J, Carmintti R, Joulain K, Mulet J P, Mainguy S and Chen Y 2002 *Nature* **416** 61

[8] Anderson M S 2003 *Appl. Phys. Lett.* **83** 2964

[9] Oceli N and Hillenbrand R 2004 *Nat. Matter* **3** 606

[10] Chen J J, Li Z and Gong Q H 2009 *Chin. Phys.* B **18** 3535

[11] Zhang Y, Zhao Q, Liao Z M and Yu D P 2009 *Chin. Phys.* B **18** 4865

[12] He M D, Wang L L, Huang W Q, Wang X J and Zou B S 2007 *Phys. Lett.* A **360** 638

[13] Ng S S, Yoon T L, Hassan Z and Hassan H A 2009 *Appl. Phys. Lett.* **145** 535

[14] Mills D L and Maradudin A A 1973 *Phys. Rev. Lett.* **31** 372

[15] Nakayama M, Ishida M and Sano N 1988 *Phys. Rev.* B **38** 6348

[16] He M D, Wang L L, Huang W Q, Wang X J and Zou B S 2006 *Semocond. Sci. Technol.* **21**1584

[17] Seo H C, Patrick C, Cho H I, Lee J H and Kim K 2008 *Appl. Phys. Lett.* **93** 102102

[18] Deutsch T G, Koval C A and Turner J A 2006 *J. Phys. Chem.* B **110** 25297

[19] Zhang D H, Liu W, Wang Y, Chen X Z, Li J H, Huang Z M and Zhang S S Y 2008 *Appl. Phys. Lett.* **93** 131107

[20] Galtrey M J, Oliver R A, Kappers M J, Humphreys C J, Clifton P H, Larson D, Saxey D W and Cerezo A 2008 *J. Appl. Phys.* **104** 013524

[21] Taylor D W 1988 *Optical Properties of Mixed Crystals* (Amsterdam: NorthHolland) Chap. 2

[22] Chang I F and Mitra S S 1971 *Adv. Phys.* **20** 359

[23] Born M and Huang K 1954 *Dynamical Theory of Crystal Lattices* (New York: Oxford University Press) p82

[24] Liang X X and Ban S L 2004 *Chin. Phys.* **13** 71

[25] Liang X X and Yang J S 1996 *Solid State Commun.* **100** 629

[26] Adachi S 1985 *J. Appl. Phys.* **58** R1

[27] Kartheuser E 1973 *Polarons in Ionic Crystals and Polar Semiconductors* (Amsterdam: NorthHolland) p718

[28] Strite S and Morkoc H 1992 *J. Vac. Sci. Technol.* B **10** 1237

[29] Bao J and Liang X X 2008 *J. Appl. Phys.* **104** 033545